CHARACTERISING LONG WAVE AGITATION IN THE PORT OF NGQURA USING A BOUSSINESQ WAVE MODEL

Duncan Stuart[1], Geoffrey Toms[2], Stephen Luger[1] and Marius Rossouw [3]

This paper summarises an investigation of long waves at the port of Ngqura, South Africa. An analysis of simultaneous wave measurements from both outside and inside the port has provided insight into long wave agitation at the port. The analysed wave data were also used to calibrate a Boussinesq wave model. It was found that the geometry of the port induced standing long waves at certain resonant frequencies. The resonant long waves were further identified and visualised over the full port domain by use of the calibrated Boussinesq wave model, with a white noise signal as input. Reflections from the adjacent beach as well as simultaneous multiple resonant modes within the port were found to provide complex oscillation characteristics which this study was able to describe, facilitated by three-dimensional temporal spectrograms and band-pass filtering techniques.

Keywords: Port of Ngqura; long waves; infra-gravity waves; resonance; Boussinesq; seiche; white noise simulation

INTRODUCTION

Port of Ngqura

The port of Ngqura is a new port which became operational in October 2009. The port, located on the east coast of South Africa in Algoa Bay, is shown in Figure 1. Since its first operational winter occasional excessive vessel motions have interrupted container shipping operations and in some instances this has led to mooring line failure. One component contributing to the excessive motions may be the presence of seiching in the port, resonating long waves. This paper documents and investigates various aspects of long wave penetration into the port and subsequent resonance in the vicinity of the problem berths.

The problem container berths are named D100 and D101 both are indicated in Figure 1 below. Also shown in the figure are the positions of the wave recording instruments that supplied data to this study. The Long Wave Recorder (LWrec) is positioned opposite berth D100 and the RBR 1 and S4DW are positioned off the main breakwater.

Figure 1. The port of Ngqura on the East coast of South Africa. The location of instruments and berths are indicated.

[1] PRDW, 5th Floor Safmarine Quay, Clock Tower Precinct, Victoria and Alfred Waterfront, Cape Town, South Africa.
[2] Chair Port & Coastal Eng., University of Stellenbosch, Private Bag X1, Matieland 7602, Stellenbosch, South Africa.
[3] CSIR, 11 Jan Celliers Street, Stellenbosch, South Africa.

Seiches and Long Waves on the South African Coast

South Africa has been the subject of a number of studies regarding long waves and seiching, in particular because the port of Cape Town in the 1950's was severely affected by seiching. Wilson (1953, 1954 & 1957) performed a number of studies investigating the seiching and potential forcing mechanisms at the port of Cape Town. Darbyshire & Darbyshire (1964) followed on Wilson's work applying the latest long wave theory at the time with use of new long wave measurements. Botes *et al*. (1982, 1984) used a relatively simple model, with regards to physical process modelling, in order to analyse the port of Cape Town and other smaller local ports. They were one of the first to use a white noise spectrum for input and subsequent post processing.

More recently Rossouw *et al*. (2013) reported on long wave characteristics on the South African coastline and a long wave forecasting algorithm in use at the port of Ngqura. Terblanche and van der Molen (2013) have linked long wave modelling to a vessel motion model in order to test various mooring systems at the port of Ngqura.

DATA

Data Description

A large amount of historical wave data was available for this study, the majority of which had already been analysed and reported on previously (PRDW, 2005). In addition, more recent wave measurement records were available which included simultaneous measurements from outside and inside the port; a detailed analysis was performed on this data to gain insight into the effect of the port on long wave energy. The data sets are described below:

Outside the port.

- Historic S4DW measurements: 1997/11/14 until the 2008/07/23 (~12 years)

Simultaneous measurements, outside and inside the port.

- RBR1 vs. LWrec: 2012/07/23 to 2012/07/31 (8 days)
- S4DW deployment 1 vs. LWrec: 2011/07/27 to 2011/08/24 (28 days)
- S4DW deployment 2 vs. LWrec: 2011/10/03 to 2011/11/06 (34 days)

The S4DW p-u-v (pressure and current velocity vectors u, v) directional wave-current meter (Model S4DW of InterOcean Systems of San Diego USA) was used in dual mode in order to record both long and short waves simultaneously. Short and long waves were defined in periods between 5 s to 30 s and 30 s and 600 s, respectively. The S4DW was installed near the entrance of the port of Ngqura, 1.7 m above the seabed in a depth of ~16.5 m below chart datum as shown in Figure 1.

The RBR instrument was deployed in a similar position as the S4DW instrument in a depth of approximately 18 m, 0.6 m above the seabed. The RBR instrument only provided pressure measurements.

Inside the port continuous water level measurements were measured on a LOG_aLevel ultrasound instrument from General Acoustics, referred to as LWrec (position also shown on Figure 1).

Data Analysis

Measurement Correlations outside the Port

Analysis of the historic S4DW long and short wave measurements outside the port revealed the exceedances of the long waves and the correlation between significant short and long wave heights. Figure 2 shows the general correlation between the significant short and long wave heights. The gradient of the linear trend line fitted to the data is 0.082 showing that on average the significant long wave height is 8% of the significant short wave height. The data scatter fits well between the 0.15 and 0.5 gradient lines giving a good indication of the extremities of the correlation i.e. the correlation of short to long wave height is most often between 5% and 15%.

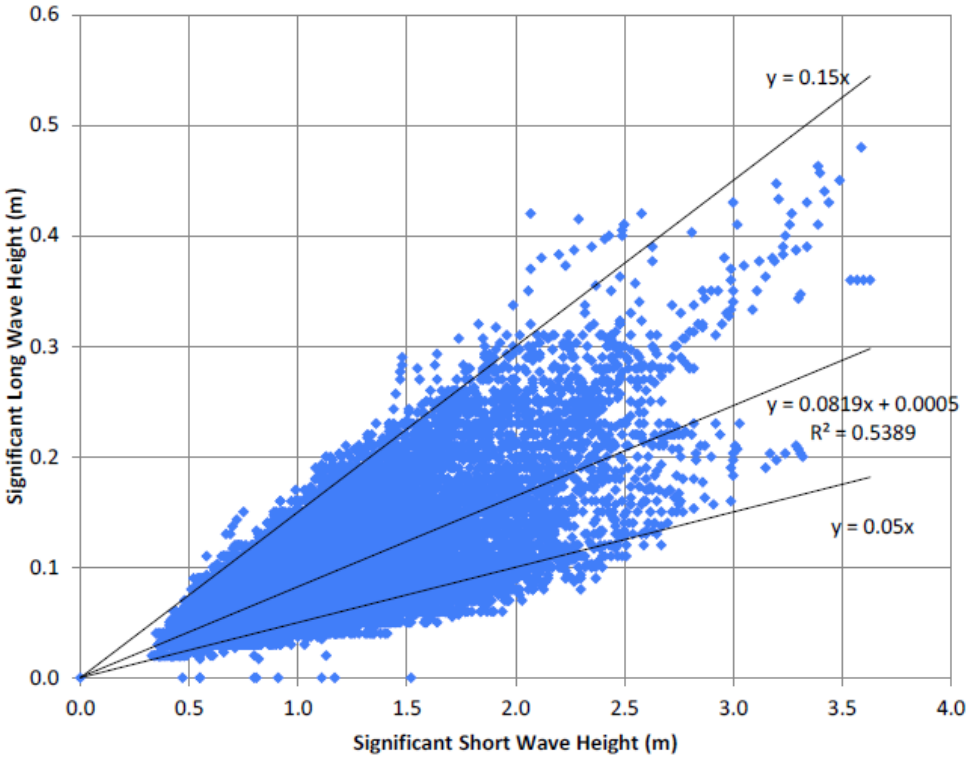

Figure 2. Correlation of long wave with short wave heights. Measurements from historic S4DW data set.

Figure 3 shows an example of the correlation of significant long wave height to short wave height in time series format. The long wave and short wave curves are from the recent S4DW data set and are measured by the same instrument. The axis of the long wave height data series, shown on the right hand side, is 8% of the short wave axis; this ratio is based on the correlation figure above (Figure 2). The obvious trend is the correlation of the short and long wave heights; the two series match each other closely over the entire duration. This type of figure was presented for the historic S4DW data in the Ngqura Port Coastal Processes report (PRDW, 2001) with very similar trends.

An important observation concluded from Figure 2 and Figure 3 is that the long wave energy corresponds to the short wave energy; hence it is concluded that the long wave energy at the port of Ngqura is predominantly generated from short waves, either through set down or nearshore breaking processes. Furthermore, on average, based purely on wave height correlation, the significant long wave heights appear to be approximately 8% of the simultaneous significant short wave heights.

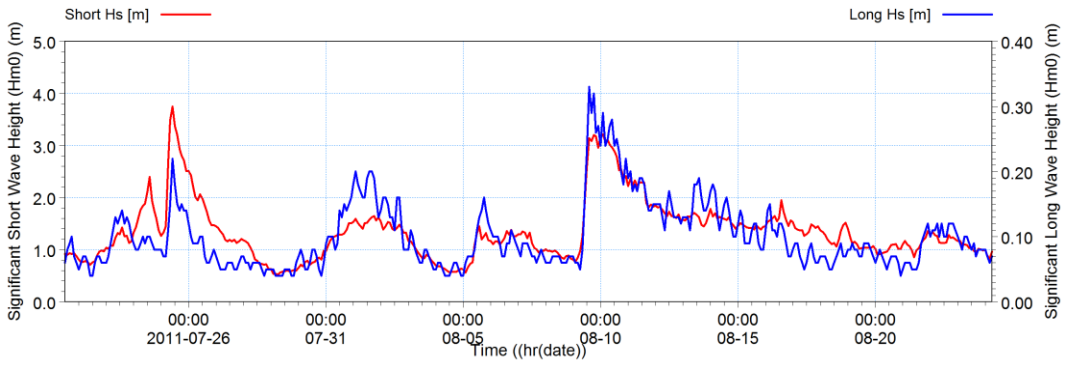

Figure 3. Comparison of short and long period significant wave heights. Long period axis is correlated to short wave height by 8%. Short and long period measurements are from the S4DW instrument outside the port.

Measurement Correlations between the Outside and Inside of Port

Figure 4 shows the correlation of significant long wave height measurements between the outside and inside of the port. All three simultaneous data sets as mentioned above were used. The plot (Figure 4) shows a linear tend between the significant long wave heights outside and inside of the port. The linear trendline fitted to the data has an R^2 value of 0.7 showing the line has a fairly good fit to the data. The equation of the line shows that on average the significant long wave height outside the port is reduced by only 10% once it reaches the inside of the port. In other words, the average long wave agitation coefficient for the port of Ngqura, based on these measurements, is 0.9. In comparison the short wave agitation coefficient for Ngqura is approximately 0.15.

The significant difference between the ability of the port to dissipate long wave energy and short wave energy highlights the difficulty in port design in reducing long wave penetration.

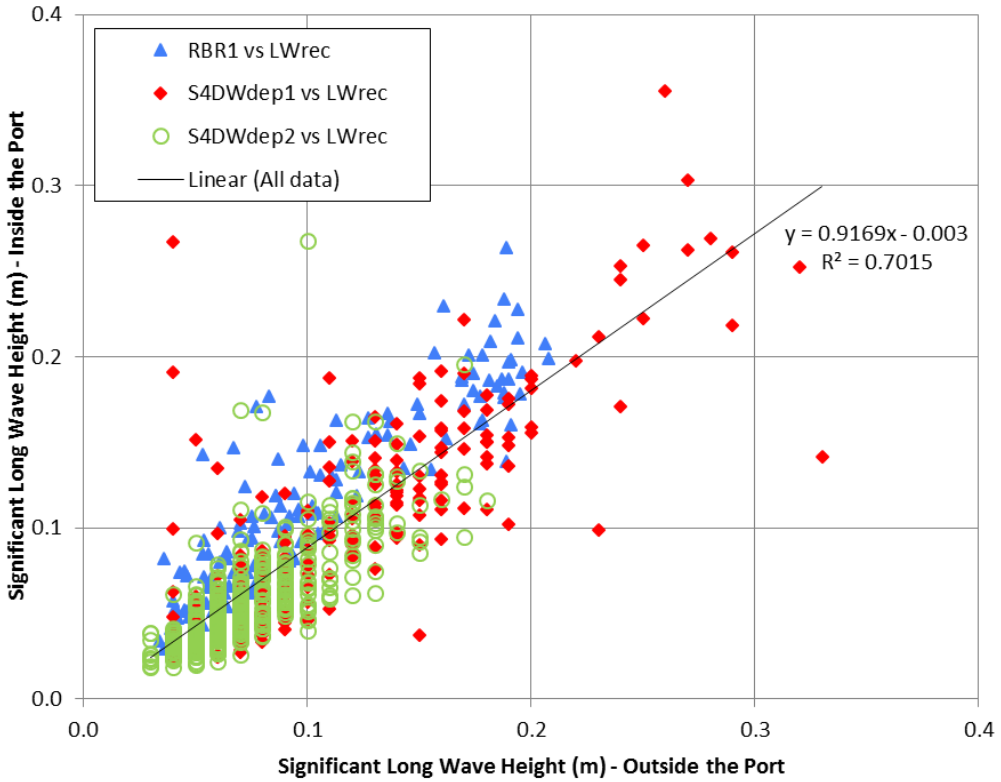

Figure 4. Correlation of significant long wave heights between the outside and inside of the port. Data consists of three separate data sets.

By comparing the spectra from inside and outside the port it is possible to see how energy may be amplified at specific frequencies once entering the port. It is the resonance at frequencies corresponding to the natural frequencies of the moored vessels that is typically more critical for vessel motion than just the significant long wave height.

Figure 5 and Figure 6 show 3D temporal spectrograms over the duration of a relatively extreme event from 2011/08/08 to 2012/08/18. The peak event parameters outside the port were $H_{m0:HF}$=3.2 m, $H_{m0:LF}$=0.29 m and $T_{p:HF}$=12 s. A temporal spectrogram essentially adds a third axis to the standard 2D spectra, a time axis. The temporal spectrogram therefore shows how the sea state, in spectral form, develops over the duration of an event rather than the spectrum at just the peak of an event. By comparing the spectrograms, the effect of the port on long wave energy is evident.

In Figure 5, showing the long wave spectra outside the port, the long wave spectra over the entire event duration are fairly flat without prominent peaks at any specific periods. By comparison, in Figure 6, which shows the long wave spectra inside the port, there are clearly

defined peaks of spectral density in certain period bands. Note that the spectral density and time axis are the same scale and are therefore directly comparable, however, the period axes differ.

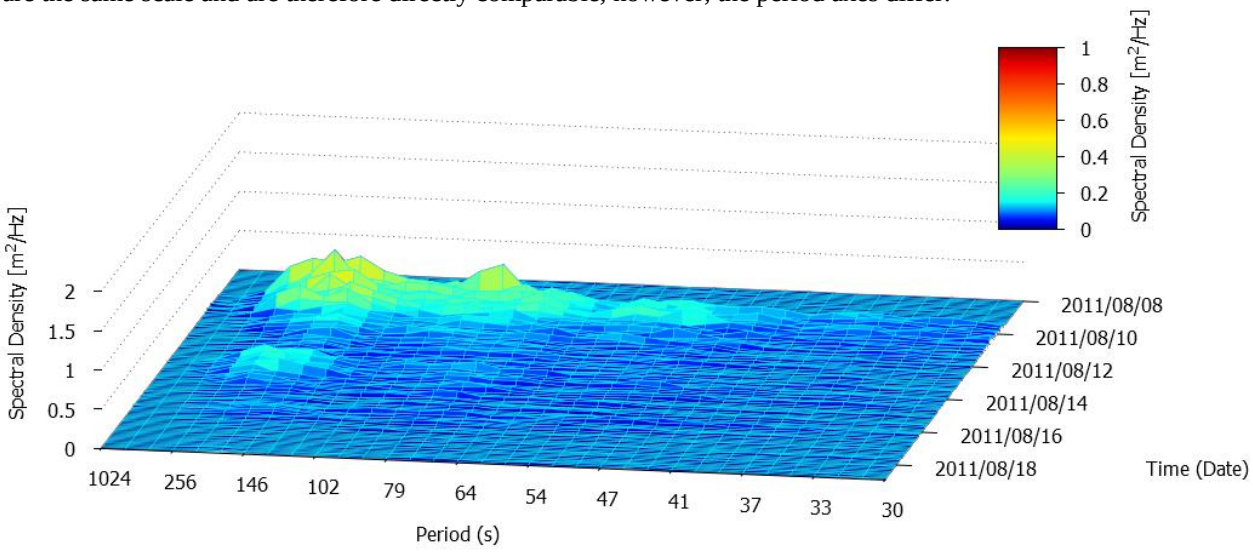

Figure 5. 3D Temporal spectrogram (spectral energy-frequency-time) variation, long wave periods only – (2011/08/08 to 2011/08/18). Measured outside the port with the S4DW.

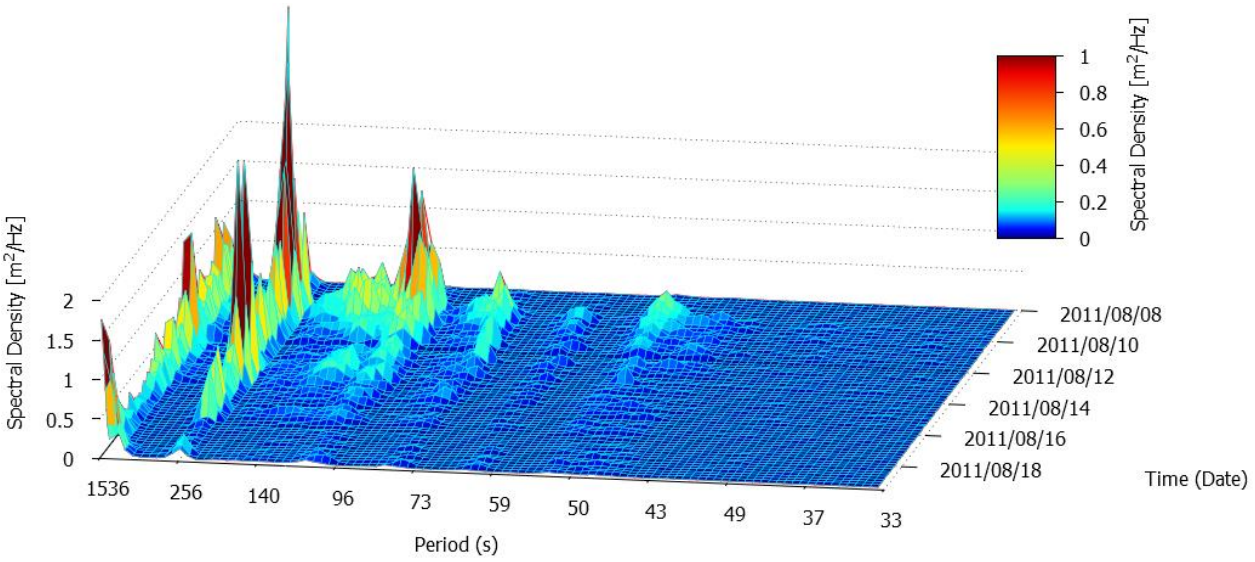

Figure 6. 3D Temporal spectrogram (spectral energy-frequency-time) variation, long wave periods only – (2011/08/08 to 2011/08/18). Measured inside the port with the LWrec.

By analysing several events using both 3D and 2D temporal spectrograms it was found that although the energy outside the port was fairly uniformly spread over the frequency range, the energy inside the port was consistently amplified at discrete period intervals, namely:

45 s to 55 s, 59 s to 70 s, 75 s to 90 s, 100 s to 160 s, 250 s to 260 s, 1000 s[4]

[4] It is noted that the wave record length is not of sufficient length to accurately define the 1000 s resonance period however subsequent white noise simulations identified the Helmholtz frequency of the port at ~820 s thus it has been included here.

BOUSSINESSQ MODEL CALIBRATION

Introduction

In order to investigate the propagation of long waves into a port, a number of complex wave phenomena need to be accurately modelled. These include shoaling, refraction, diffraction and partial reflection of irregular, finite amplitude waves propagating over complex bathymetries (Gierlevsen et al., 2001). The Boussinesq Wave Module of MIKE by DHI (MIKE 21 BW) incorporates enhanced Boussinesq equations that adequately model the phenomena mentioned above and for this reason the model was utilized in this study.

A detailed description of the enhanced Boussinessq equations and the numerical methods used to solve them are included in DHI (2012).

Methodology

The calibration of the model was aimed at setting up the model as accurately as possible and adjusting necessary parameters realistically, to achieve a result similar to the measurements available.

The initial step in the calibration process was to ensure that the results given by the model obeyed the expected trends and outputted physically plausible results. This included inspection of 2D plots showing the significant short wave height across the domain, and surface elevation animations showing the propagation of short waves, an example is shown in Figure 7. The next step was to compare the measured wave heights with the modelled wave heights.

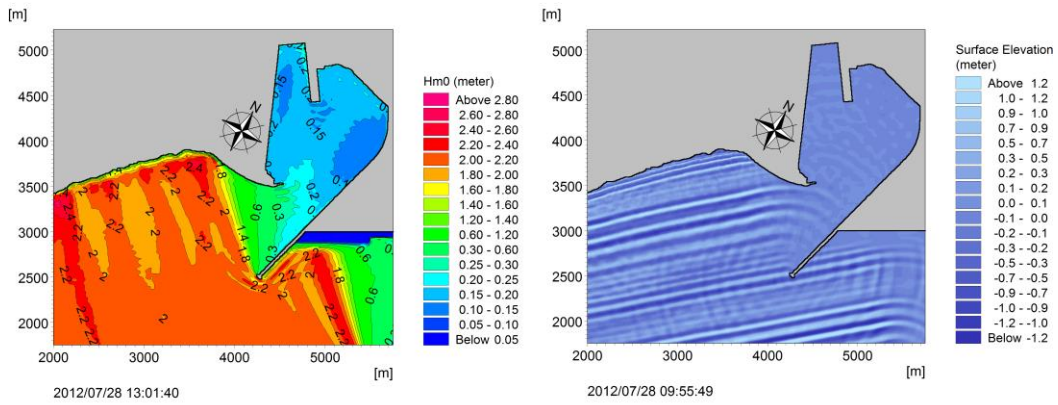

Figure 7. Example of modelled significant short wave height (left pane) and instantaneous surface elevation (right pane).

Surface elevation measurements outside the port were available, sampled at a sufficient sampling interval to accurately resolve the short and long waves for a 4.5 hour period. Inside the harbour simultaneously measured surface elevation measurements were available; however, the measurements were only sampled at a sampling interval sufficient to resolve the long waves. Therefore, in the calibration process, comparison of short wave heights was not possible (except on the input boundary) and only long wave heights could be compared inside the port. The surface elevation measurements were used as input for the model in order to conserve the phasing of the waves, the effect of groups, and hence, conserve the bound long wave energy as accurately as possible.

The most detailed calibration output for comparison between the model and measurements was direct spectral comparison of the long wave spectra inside the port, at the location of the long wave recorder.

Summary and Results

Two events were modelled during the calibration process to ensure the model was not biased for a specific event and that the chance of using an event including measurement anomalies was reduced.

For each event the long wave height from the model was compared with the measured data. All the data was extracted from the position of the Long Wave Recorder within the port basin (Figure 1). The modelled events compared well with the measured significant long wave height as

the difference was less than 0.02 m in each case. The measured significant long wave heights for the two events were 0.17 m and 0.19 m.

Figure 8 shows an example of the comparison of long wave spectra produced from the model and analysis of the measurements. The long wave spectra comparisons showed close alignment.

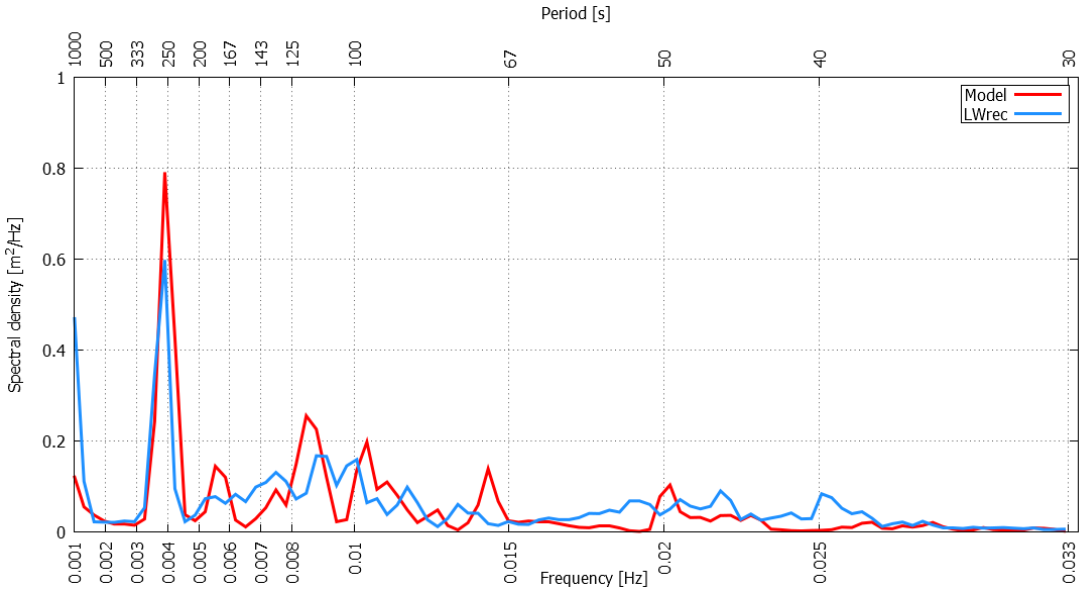

Figure 8. Long wave spectra comparison, model vs. LWrec for event of 2012/07/28 14h30. Model $H_{m0:LF}$ = 0.17 m, LWrec $H_{m0:LF}$ = 0.17 m.

WHITE NOISE SIMILATION

Introduction

The data analysed and the event modelled above, although typical, do not necessarily represent all events. A more generic white noise simulation approach was applied in order to identify and confirm all the resonance frequencies of the port. This approach does not rely on specific input data which could contain existing energy peaks that could have forced less characteristic resonance periods and missed others.

As no measurements are necessary to define the input conditions for the white noise simulation the model could be simulated for an extended period of time. The extended period of time allowed the spectral analysis of the results to be performed on a much larger output data set than was previously possible. Hence, a higher resolution spectrum with a greater degree of confidence could be obtained.

White Noise Input

The white noise approach involves forcing the boundary of a Boussinesq wave model with a flux generated from a white noise spectrum. A white noise spectrum is characterised as having equal amounts of energy at every period in a defined frequency range. In this study, the white noise spectrum frequency range was set between 30 and 1000 seconds. This is equivalent to propagating waves of every defined period into the model domain in one run. Although this is a synthetic exercise it has the following advantages when considering long wave resonance in a port:

- By analysing various areas in the port it is possible through spectral analysis to identify the resonance periods of the port.
- The method allows for reduced run times as many wave periods are included in one run.
- No long wave measurements are required for this approach.

It is important to realize that the white noise spectra represents a synthetic sea state and for that reason may only be used to indicate potential resonating frequencies.

The white noise modelling approach has been well documented and used successfully to identify port resonance, e.g. (Kofoed-Hansen *et al*., 2005) and (Gierlevsen *et al*., 2001).

Results – Spectrum

Figure 9 shows the output spectrum from the white noise simulation. The time series used for the spectral analysis was outputted from the position of the long wave recorder inside the port. The following resonance period intervals are clearly defined: 42 s to 49 s, 52 s to 58 s, 67 s to 71 s, 85 s to 105 s, 115 s to 125 s, 155 s to 200 s and 240 s to 260 s. These period intervals fall within the period ranges identified in the measured data analysis.

In addition to the white noise model output spectrum, three maximum spectra envelopes from storm events have been shown, in order to allow a quasi-validation of the results. Each envelope represents the measured maximum spectral density levels occurring during the full duration of a fairly significant storm event, with the 2011/08/10 event representing the largest storm event of the three.

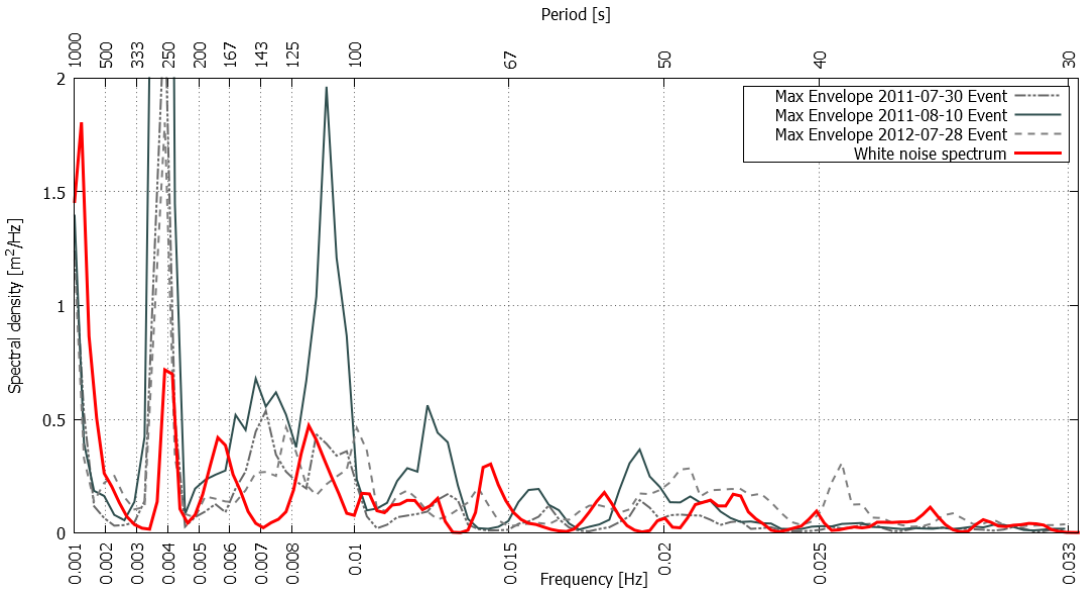

Figure 9. Long wave white noise results spectrum vs. long wave maximum spectra envelopes for three events.

In general the white noise model output (red) has lower energy than the three event envelopes which is expected because the events were high energy events and the event spectra (grey) represent the maximum energy in each frequency over an entire storm duration.

Encouragingly, the strongest two resonant modes viz. ~800 s and 250 s are shared by all the events and the white noise simulation. The third and fourth highest peaks lie within an energetic period shared by the three events between 100 s and 200 s. The remaining white noise resonance peaks do not look unnatural with regard to the variability displayed by the event measurements; it also appears that no significant resonant mode shared by all the events is missed in the white noise simulation. Thus the quasi-validation adds a degree of confidence to the white noise simulation results and logically to the identification of the resonance mechanisms as well.

Results – Band-pass filtering

In order to visualise and gain better insight into the factors driving resonance in the port the resonance period intervals have been looked at more closely. By band-pass filtering the surface elevation output files from the white noise simulation, it is possible to look at the long wave energy and surface elevation in specified period intervals. This technique allows for the visualisation of the position of nodes and anti-nodes as well as the surface elevations for specific period intervals.

Figure 10 shows an investigation of the long wave energy between 230 s to 270 s. In the left pane, the position of long wave energy is shown, in the right pane, a snapshot of the instantaneous surface elevation. The lower pane of the figure shows a surface elevation envelope corresponding to the section indicated on the surface elevation pane above. The energy and surface elevation plots

are defined by cool and warm colours, for the energy plot warm colours are high energy and cold colours show less energy. For the surface elevation plot warm colours indicate a rise in water surface and cold colours a drop below the mean water level. The long wave energy pane on the left indicates the position of nodes and anti-nodes. The surface elevation pane on the right of the figure shows the synchronization of the nodal pattern; the contrast of warm and cool colours shows which anti-nodes are above the mean water level when the others are below the mean water level.

Thus with the help of Figure 10 the 230 s to 270 s resonance interval may be described as being driven by two mechanisms acting together; the "fundamental mode" of an open ended basin coupled with the "fundamental mode" of a closed basin. The open basin mechanism is driven simply by the length of the rectangular shaped basin enclosing the D100 and D101 berths which corresponds approximately to a quarter of a wave length (axis shown by profile A-B). The anti-node positioned at the top of the basin is further amplified by a coupling with the fundamental mode of a closed basin mechanism. The secondary mechanism resonates a half wave length between the top of the D series basin and the spending beach positioned at the eastern side of the port (axis shown by curved magenta line). The two mechanisms resonate in sync with one another i.e. as the surface elevation within the rectangular basin rises it is driven by both mechanisms and vice a versa.

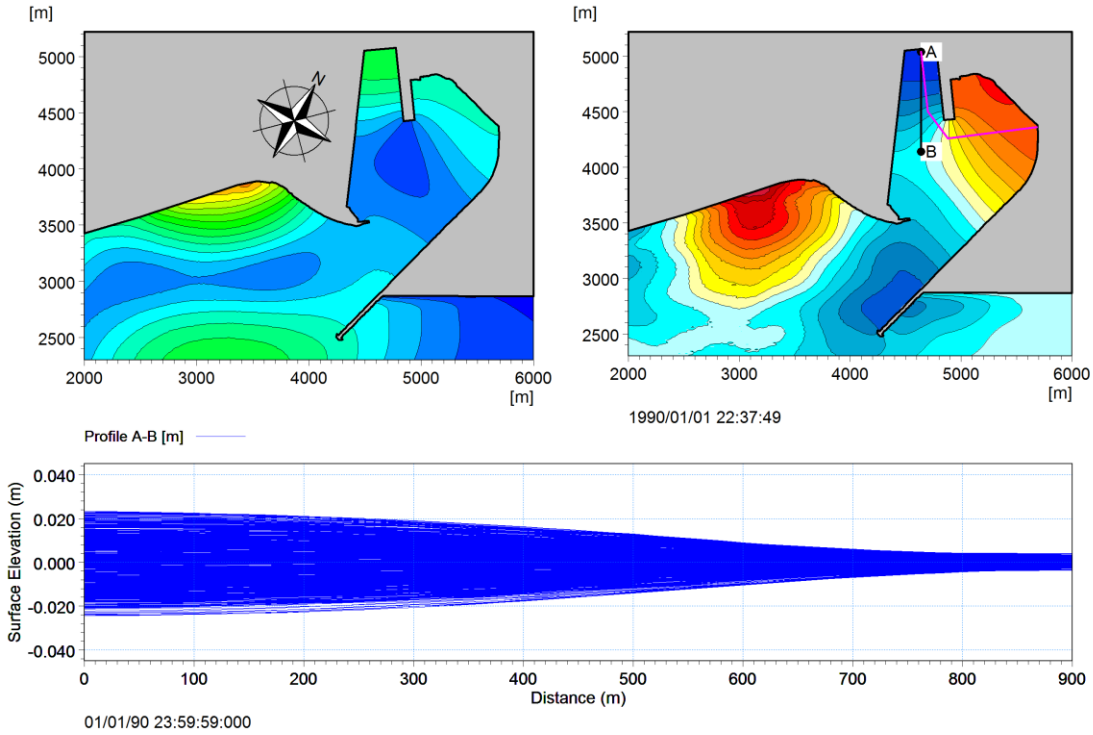

Figure 10. 230 s to 270 s - Short Open Basin coupled with Short Closed Basin – Fundamental Modes. Left: normalized long wave energy, Right: surface elevation, Lower: surface elevation profile envelope along line A-B.

By performing a similar band-pass filtering exercise for the remaining resonant periods all the nodal patterns of the port can be visualised. Figure 11 shows a summary of the nodal patterns for the resonant periods.

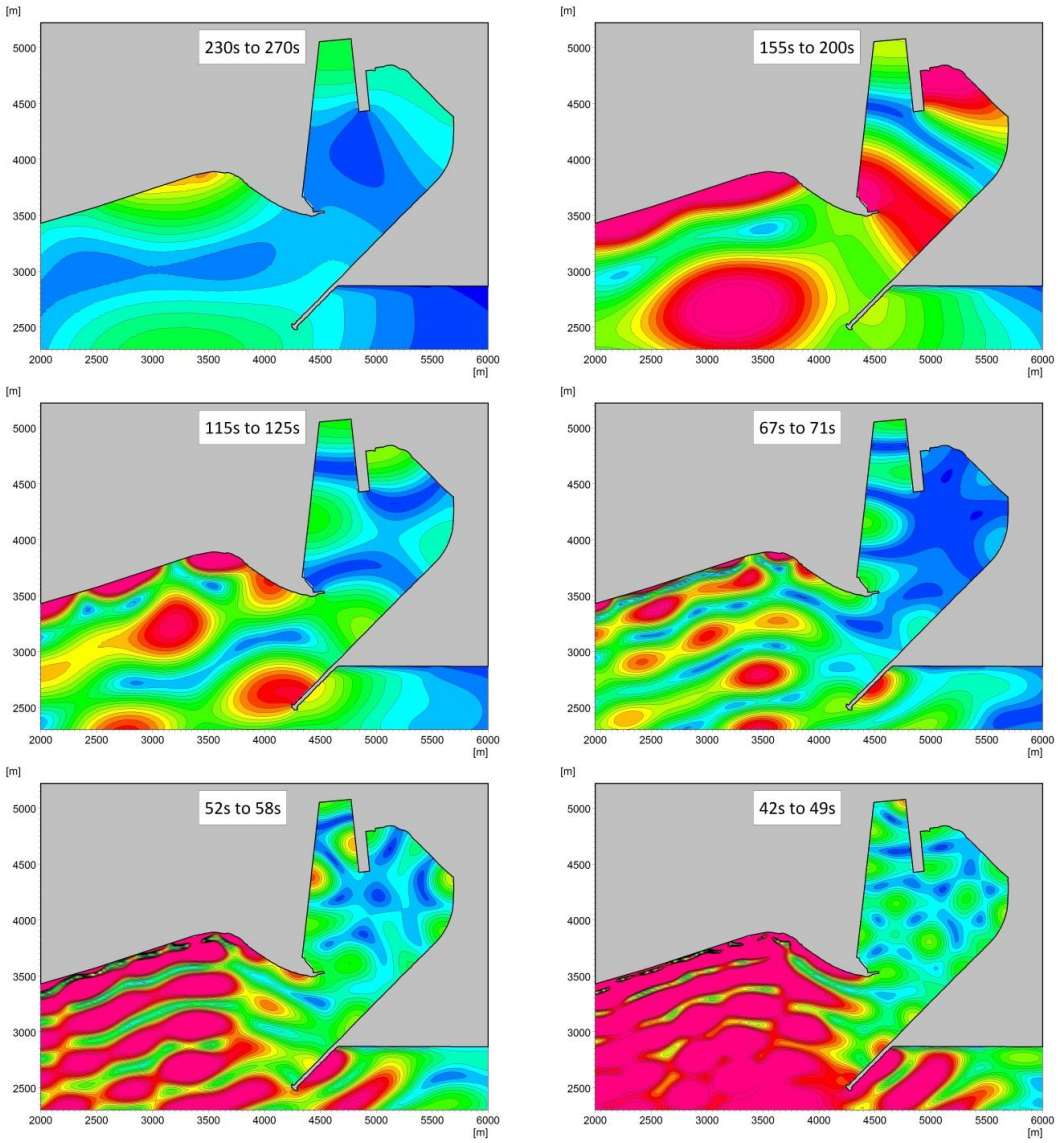

Figure 11. Summary of resonant long wave energy periods at the port of Ngqura, warm colours indicate anti-nodes, cold colours indicate nodes.

CONCLUSIONS

An in-depth analysis of wave measurements, both inside and outside the port, was used to initially characterise long waves at the port. The data analysis showed that the long wave heights outside the port were correlated to the coincident short waves. On average the significant long wave heights were approximately 8% of the short wave heights. This correlation and a close inspection of direct time series comparisons suggests that the majority of the long wave energy is linked to the short wave energy; hence the term "bound long waves" applies.

The white noise simulation compared well with measurements and the wave penetration models. Band-pass filtering of the model results identified the position of the nodal patterns for specific resonance periods; this helped clarify how the port geometry contributes to each resonance period. The predominant resonance periods found in the port were as follows: 42 s to 49 s, 52 s to 58 s, 67 s to 71 s, 85 s to 105 s, 115 s to 125 s, 155 s to 200 s and 240 s to 260 s

ACKNOWLEDGMENTS

This paper summarises a thesis presented by the lead author as a partial requirement for attaining a MSc. in port and coastal engineering at the University of Stellenbosch. I would like to thank PRDW, my employer, for financing my studies and attendance to ICCE 2014. Thanks to the co-authors for their valuable inputs, guidance, support and provision of data. In addition DHI for providing a student license for the Mike by DHI suite of software.

REFERENCES

Botes, W. A., Russel, K. S., & Huizinga, P. (1982). Resonance in South African Harbours. *Proceedings of 18th Conference on Coastal Engineering.* Cape Town: ASCE.

Botes, W. A., Russel, K. S., & Huizinga, P. (1984). Model Harbour Seiching Compared to Prototype Data. *Proceedings of 19th Conference on Coastal Engineering.* Texas: ASCE.

Darbyshire, J., & Darbyshire, M. (1964). Range Action in Table Bay Harbour. *South African Journal of Science*, 173-182.

DHI. (2012). *Mike 21 BW, Boussinesq Waves Module, Scientific Documentation.* Copenhagen, Denmark: Danish Hydraulics Institute.

Gierlevsen, T., Hebsgaard, H., & Kirkegaard, J. (2001). Wave Disturbance Modelling in the Port of Sines, Portugal - with special emphasis on the long period oscillations. *International Conference on Port and Maritime R&D and Technology.* Singapore.

Kofoed-Hansen, H., Kerper, D. R., Sørensen, O. R., & Kirkegaard, J. (2005). Simulation of Long Wave Agitation in Ports and Harbours using a Time-domain Boussinesq Model. *Proceedings of Fifth International Symposium on Ocean Wave Measurement and Analysis-Waves.* Madrid, Spain.

PRDW. (2005). *Coega Port: Maritime Works. Sub-Task J: Coastal Processes. Wave Data Recorded at S4. Interim Report No. 256/J03/s006 Rev 03.* Not published.

Rossouw, M., Terblanche, L., & Moes, J. (2013). General characteristics of long waves around the South African Coast. *Coasts & Ports 2013 Conference : 21st Australasian Coastal and Ocean Engineering Conference and the 14th Australasian Port and Harbour Conference* (pp. 653-658). Sydney: Barton, A.C.T.: Engineers Australia.

Terblanche, L., & van der Molen, W. (2013). Numerical modelling of long waves and moored ship motions. *Coasts and Ports 2013: 21st Australasian Coastal and Ocean Engineering Conference and the 14th Australasian Port and Harbour Conference* (pp. 757-762). Sydney: Barton, A.C.T.: Engineers Australia.

Wilson, B. W. (1953). Table Bay as an oscillating basin. Minneapolis: Proc. of Joint Convention of International Assoc. Hydraulic Research and Am. Soc. Civ. Engrg.

Wilson, B. W. (1953). The mechanism of seiches in Table Bay Harbour, Cape Town. *Proceedings of 4th Conference on Coastal Engineering.* Berkeley: Chicago.

Wilson, B. W. (1957). Origin and effects of long period waves in ports. *Proc. 19th Navigation Congr.*

Wilson, B. W. (1972). Seiches. In *Advances in Hydroscience* (pp. 1-94). California.